HOSTED BY

Available online at www.sciencedirect.com
ScienceDirect
Journal of Radiation Research and Applied Sciences
journal homepage: http://www.elsevier.com/locate/jrras

Europium doped di-calcium magnesium di-silicate orange–red emitting phosphor by solid state reaction method

*Ishwar Prasad Sahu**, *D.P. Bisen*, *Nameeta Brahme*

School of Studies in Physics & Astrophysics, Pt. Ravishankar Shukla University, Raipur, C.G., 492010, India

ARTICLE INFO

Article history:
Received 27 October 2014
Received in revised form
28 January 2015
Accepted 18 February 2015
Available online 14 March 2015

Keywords:
$Ca_2MgSi_2O_7:Eu^{3+}$
TEM
Photoluminescence
Long afterglow
CIE

ABSTRACT

A new orange–red europium doped di-calcium magnesium di-silicate ($Ca_2MgSi_2O_7:Eu^{3+}$) phosphor was prepared by the traditional high temperature solid state reaction method. The prepared $Ca_2MgSi_2O_7:Eu^{3+}$ phosphor was characterized by X-ray diffractometer (XRD), transmission electron microscopy (TEM), field emission scanning electron microscopy (FESEM) with energy dispersive x-ray spectroscopy (EDX), fourier transform infrared spectra (FTIR), photoluminescence (PL) and decay characteristics. The phase structure of sintered phosphor was akermanite type structure which belongs to the tetragonal crystallography with space group $P\bar{4}2_1m$, this structure is a member of the melilite group and forms a layered compound. The chemical composition of the sintered $Ca_2MgSi_2O_7:Eu^{3+}$ phosphor was confirmed by EDX spectra. The PL spectra indicate that $Ca_2MgSi_2O_7:Eu^{3+}$ can be excited effectively by near ultraviolet (NUV) light and exhibit bright orange–red emission with excellent color stability. The fluorescence lifetime of $Ca_2MgSi_2O_7:Eu^{3+}$ phosphor was found to be 28.47 ms. CIE color coordinates of $Ca_2MgSi_2O_7:Eu^{3+}$ phosphor is suitable as orange-red light emitting phosphor with a CIE value of (X = 0.5554, Y = 0.4397). Therefore, it is considered to be a new promising orange–red emitting phosphor for white light emitting diode (LED) application.

1. Introduction

Luminescent materials containing rare earth ions are able to absorb energy in the UV-regions and emit visible light. Recently, these materials have drawn increasing interest due to their promising applications in white light emitting diodes, display devices, storage bioluminescence and fluorescence labels (Sahu, Bisen, Brahme, Wanjari, Tamrakar, 2015b; Xu, Wang, Liu, Jia, & Sheng, 2014).

As a new solid state light source, the white light-emitting diodes (WLEDs) are considered to be the fourth generation general lighting devices that stands a real chance of replacing conventional lighting sources such as incandescent and fluorescent lamps due to its long lifetime, saving energy, reliability, safety and its environmental friendly characteristics (Jiao & Wang, 2012). Among the technological strategies of obtaining WLEDs, the phosphor converted (pc) emission method is the most common one, in which tricolor phosphors

* *Corresponding author*. Tel.: +91 9926993644.
E-mail address: ishwarprasad1986@gmail.com (I.P. Sahu).
Peer review under responsibility of The Egyptian Society of Radiation Sciences and Applications.
http://dx.doi.org/10.1016/j.jrras.2015.02.007

(red, green and blue) are pumped by UV InGaN chips or blue GaN chips and generate white light. At present, the commercially used green and red phosphors for NUV chips are ZnS:(Cu^{+}, Al^{3+}) and $Y_2O_2S:Eu^{3+}$, respectively. Unfortunately, both ZnS:(Cu^{+}, Al^{3+}) and $Y_2O_2S:Eu^{3+}$ show low chemical stability as they are sulfide based phosphors. Therefore, it is urgent to search for new green and red phosphors or an orange–red phosphor with high efficiency and excellent stability (Liu et al. 2014).

Generally, phosphors consist of activator and host, in order to obtain efficient red or orange–red emitting phosphor, host is another key factor (Wang, Lou, & Li, 2014). Eu^{3+} doped oxides were widely studied as efficient red emitting phosphors due to the abundant transitions from the excited $^5D_0$ level to the ^7F_J (J = 0, 1, 2, 3, 4) levels of the $4f^6$ configuration in the orange-red light area (Dong, Zhang, Zhang, Hao, & Luo, 2014; Gorller-Walrand, Fluyt, Ceulemans, & Carnall, 1995). Mellite are a large group of compounds characterized by the general formula $M_2T^1T^2{}_2O_7$, (M = Sr, Ca, Ba; T^1 = Mn, Co, Cu, Mg, Zn; T_2 = Si, Ge), have been investigated widely as optical materials. Due to their tetragonal and non-centrosymmetric crystal structure, lanthanides or transition metals can be accepted easily as constituents or dopants by the melilites, allowing the synthesis of high-quality doped single crystals. Recently, di-calcium magnesium di-silicate ($Ca_2MgSi_2O_7$) phosphor has attracted great interest due to its special structure features, excellent physical and chemical stability. They have been studied widely with Eu^{2+} doping, which shows that a green emission and long persistent luminescence by co-doping with some other rare earth ions. A calcium silicate phosphor would be ideal from the manufacturing point of view, because both calcium and silica are abundant and are relatively inexpensive (Talwar et al. 2009).

In the past, $Ca_2MgSi_2O_7$ phosphor doped with Eu^{3+} has been prepared by pulsed laser deposition method. High quality $Ca_2MgSi_2O_7:Eu^{3+}$ films phosphors were deposited on Al_2O_3 (0 0 0 1) substrates. The crystallinity, surface roughness and photoluminescence of the thin film phosphors were strongly dependent on the deposition conditions, which is the drawback of pulsed laser deposition method (Yang, Moona, Choi, Jeong, & Kim, 2012). Solid state reaction techniques is a traditional phosphors synthesis techniques is widely used to prepare silicate phosphors because samples prepared using this method have good luminescence and very good morphology, which has advantage over the pulsed laser deposition technique (Sahu, Bisen, & Brahme, 2015a, Shrivastava & Kaur, 2014).

In the present paper, we report the synthesis of europium doped di-calcium magnesium di-silicate ($Ca_2MgSi_2O_7:Eu^{3+}$) phosphor by high temperature solid state reaction method. The phase structure, crystallite size, particle size, surface morphology, elemental analysis, different stretching mode was analyzed by X-ray diffractometer (XRD), transmission electron microscopy (TEM), field emission scanning electron microscopy (FESEM) with energy dispersive X-ray spectroscopy (EDX), and fourier transform infrared (FTIR) spectra respectively. The luminescent behaviors of this phosphor were also investigated by photoluminescence (PL) and long afterglow (decay) characteristics.

2. Experimental

2.1. Material preparation

The $Ca_2MgSi_2O_7:Eu^{3+}$ phosphor was prepared by the high temperature solid state reaction method. The raw materials are calcium carbonate [$CaCO_3$ (99.90%)], magnesium oxide [MgO (99.90%)], silicon di-oxide [SiO_2 (99.99%)] and europium oxide [Eu_2O_3 (99.99%)], all of analytical grade (A.R.), were employed in this experiment. Boric acid (H_3BO_3) was added as flux. Initially, the raw materials were weighed according to the nominal compositions of $Ca_2MgSi_2O_7:Eu^{3+}$ phosphor. Then the powders were mixed and milled thoroughly for 2 h using mortar and pestle. The grinded sample was placed in an alumina crucible and subsequently fired at 1200 °C for 3 h in air. At last the nominal compounds were obtained after the cooling down of programmable furnace.

2.2. Characterization techniques

The phase structures of the prepared $Ca_2MgSi_2O_7:Eu^{3+}$ phosphor was characterized by powder X-ray diffraction analysis (XRD). XRD pattern has been obtained from Bruker D8 advanced X-ray powder diffractometer using CuKα radiation and the data were collected over the 2θ range 10–80°. Particle size of prepared phosphor was determined by TEM using TECHNAI G2. The samples required for TEM analysis were prepared by dispersing the sintered $Ca_2MgSi_2O_7:Eu^{3+}$ phosphor in methanol using an ultrasound bath technique. A drop of this dispersed suspension was put onto 200-mesh carbon coated copper grid and then dried into the air. An EDX spectra was used for the elemental analysis of the prepared phosphor (Sahu, Bisen, Brahme & Ganjir 2015c). FTIR spectra were recorded with the help of IR Prestige-21 by SHIMADZU for investigating the functional group (4000–1400 cm^{-1}) as well as the finger print region (1400–400 cm^{-1}) of sintered phosphor by mixing the sample with potassium bromide (KBr, AR grade). The PL measurements of excitation and emission spectra were recorded on a Shimadzu (RF 5301-PC) spectrofluorophotometer fitted with a sensitive photomultiplier tube. This spectrofluorophotometer provides corrected excitation and emission spectra in the 200–400 and 475–700 nm ranges, respectively. All measurements were carried out at the room temperature.

3. Results and discussion

3.1. XRD analysis

In order to determine the phase structure, powder XRD analysis has been carried out. The typical XRD patterns of $Ca_2MgSi_2O_7:Eu^{3+}$ phosphor with the standard XRD pattern is shown in Fig. 1. The position and intensity of diffraction peaks of the prepared $Ca_2MgSi_2O_7:Eu^{3+}$ phosphor were matched and found to be consistent with the standard XRD pattern (COD card No. 96-900-6941) by MATCH 2 software. The figure of merit (FOM) while matching these was 0.9759 (97%) which

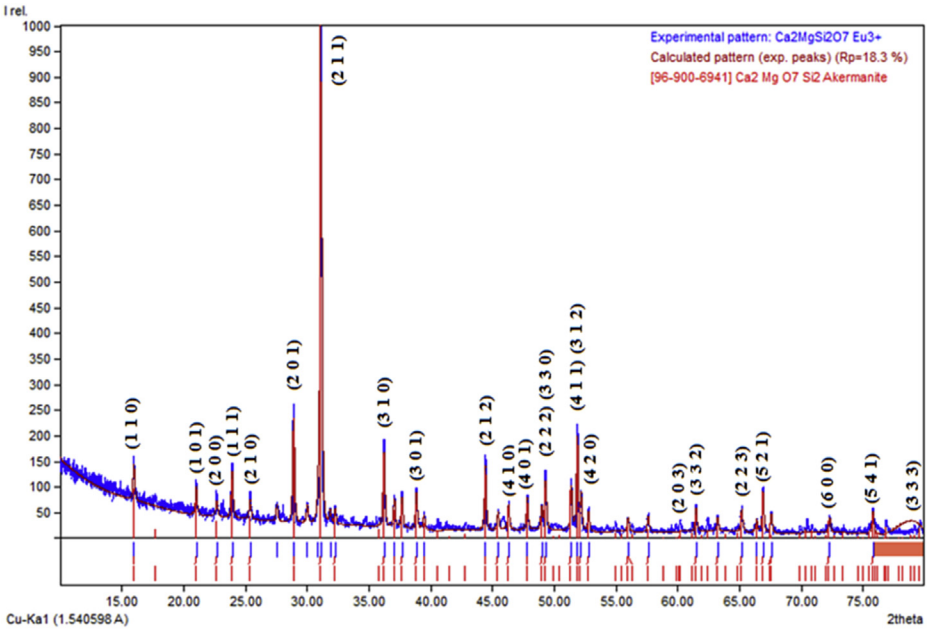

Fig. 1 – XRD patterns of $Ca_2MgSi_2O_7:Eu^{3+}$ phosphor.

illustrates that the phase of the prepared sample agrees with the standard pattern COD card No. 96-900-6941. In Fig. 1, it can be concluded that prepared samples are chemically and structurally $Ca_2MgSi_2O_7$ phosphor. The phase structure of the $Ca_2MgSi_2O_7:Eu^{3+}$ phosphor is akermanite type structure which belongs to the tetragonal crystallography with space group $P\bar{4}2_1m$ (113 space number and D^3_{2d} space group), this structure is a member of the melilite group and forms a layered compound. The lattice parameters are calculated using Celref V3. The refined values of tetragonal europium doped di-calcium magnesium silicate were found as; $a = b = 7.8470$ Å, $c = 5.0097$ Å, $\alpha = 90°$, $\beta = 90°$, $\gamma = 90°$ and cell volume $= 299.24$ (Å)^3, $Z = 2$ is nearly same [$a = b = 7.8350$ Å and $c = 5.0100$ Å, $\alpha = 90°$, $\beta = 90°$, $\gamma = 90°$ and cell volume $= 299.36$ (Å)^3, $Z = 2$], with the standard lattice parameters which again signifies the proper preparation of the discussed $Ca_2MgSi_2O_7:Eu^{3+}$ phosphor.

The average crystallite size was calculated from the XRD pattern using Debye Scherrer relation $D = k\lambda/\beta\cos\theta$, where D is the crystallite size for the (hkl) plane, λ is the wavelength of the incident X-ray radiation [CuKα (0.154 nm)], β is the full width at half maximum (FWHM) in radiations, and θ is the corresponding angle of Bragg diffraction. Sharper and isolated diffraction peaks such as $2\theta = 24.15$ (1 1 1), 29.04 (2 1 0), 31.26 (2 1 1), 36.44 (3 1 0), 38.93 (3 0 1), 44.55 (2 1 2) were chosen for calculation of the crystallite size. Based on the Debye-Scherrer's formula, the crystallite size is ~ 73 nm, 70 nm, 68 nm, 69 nm, 67 nm, 66 nm was calculated, respectively and the average crystallite size is ~68.83 nm.

3.2. *Transmission electron microscopy (TEM)*

Fig. 2 shows the transmission electron microscopy (TEM) image of $Ca_2MgSi_2O_7:Eu^{3+}$ phosphor. From TEM image, it is seen that the, due the high temperature synthesis, the agglomeration of phosphor particles were observed. TEM images shows that the shape of the particle is tetragonal structure and particle size ranges in between 200 and 400 nm. So we conclude that, transmission electron microscopy results are in good agreement with the result of the XRD studies.

3.3. *Field emission scanning electron microscopy (FESEM)*

It is known that the luminescence characteristics of phosphor particles depend on the morphology of the particles, such as size, shape, size distribution, defects, and so on. The surface morphology of the $Ca_2MgSi_2O_7:Eu^{3+}$ phosphor is shown in

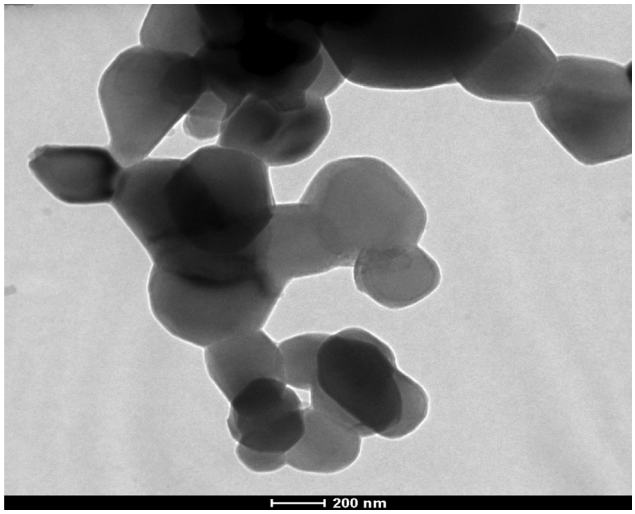

Fig. 2 – TEM image of $Ca_2MgSi_2O_7:Eu^{3+}$ phosphor.

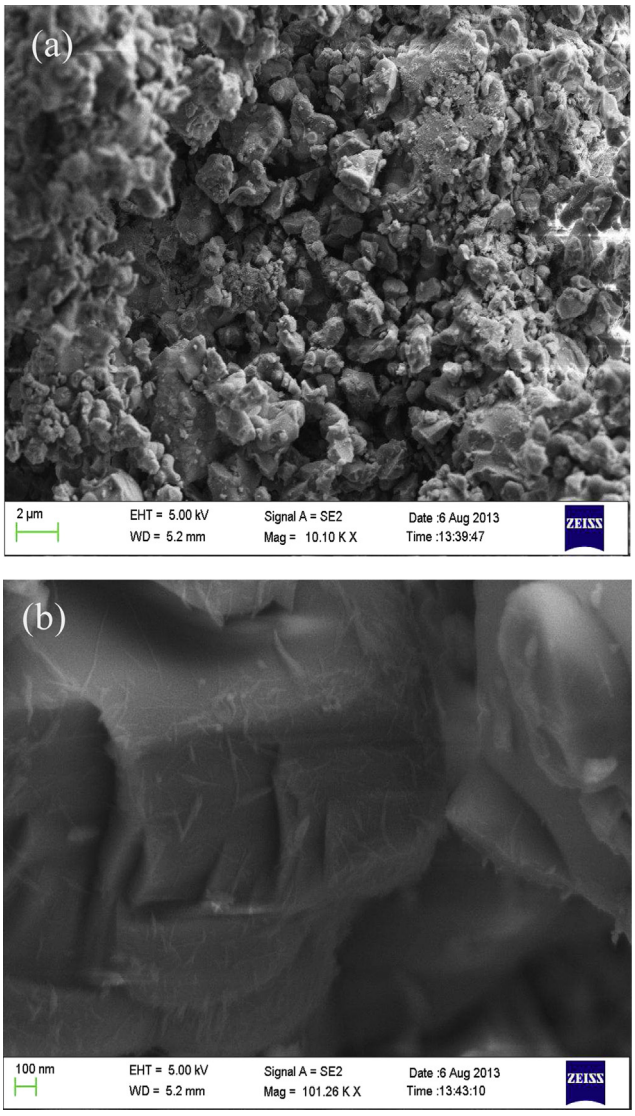

Fig. 3 – (a, b) FESEM image of $Ca_2MgSi_2O_7:Eu^{3+}$ phosphor.

Fig. 3(a, b) with different magnification. The surface morphology of the particles was not uniform and they aggregated tightly with each other. From the FESEM image, it can be observed that the prepared sample consists of particles with different size distribution. In addition, there are some big aggregates is also present due to high temperature heat treatment.

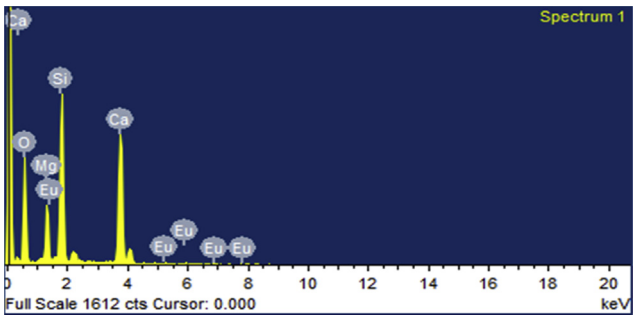

Fig. 4 – EDX spectra of $Ca_2MgSi_2O_7:Eu^{3+}$ phosphor.

3.4. *Energy dispersive X-ray spectroscopy (EDX)*

The chemical composition of the powder sample has been measured using EDX spectra. EDX is a standard procedure for identifying and quantifying elemental composition of sample area as small as a few nanometers. The existence of europium (Eu) is clear in their corresponding EDX spectra. Their appeared no other emission apart from calcium (Ca), magnesium (Mg), silicon (Si) and oxygen (O) in $Ca_2MgSi_2O_7:Eu^{3+}$ EDX spectra of the phosphor. In EDX spectra, the presence of Ca, Mg, Si, O and Eu, intense peak are present which preliminary indicates the formation of $Ca_2MgSi_2O_7:Eu^{3+}$ phosphor in Fig. 4.

3.5. *Fourier transform infrared spectra (FTIR)*

The FTIR spectra has been widely used for the identification of organic and inorganic compounds. Fig. 5 shows the FTIR spectra of $Ca_2MgSi_2O_7:Eu^{3+}$ phosphor. In observed IR spectrum, the absorption bands of silicate groups were clearly evident. An intense band centred at 974.14 cm^{-1} is assigned due to Si–O–Si asymmetric stretch, bands at 646.29 cm^{-1} to Si–O symmetric stretch. Bands at 588.71 and 481.56 cm^{-1} are assigned to Si–O–Si vibrational mode. Furthermore, in keeping with the absorption bands, posited at 1010.92, 945.36 and 687.87 cm^{-1} can be ascribed to the presence of SiO_4 group. The band centred at 1783.38 cm^{-1} can be attributed to the presence of small amount of calcite (Gou, Chang, & Zhai, 2005).

The FTIR spectrum of $Ca_2MgSi_2O_7:Eu^{3+}$ phosphor contain clearly exhibited bands in the region (3429.43 cm^{-1}) of hydroxyl group show the stretching vibration of O–H groups. The hydroxyl group in sintered phosphor is might be due to presence of moisture through environment. The asymmetric stretching of (CO_3^{2-}) carbonates can be observed in the range of 1900–1700 cm^{-1} (Sahu, Bisen, & Brahme, 2014b). The weak shoulders, which corresponds to the out of plane bending of appears at ~1861.65 cm^{-1}. These bands are due to a slight

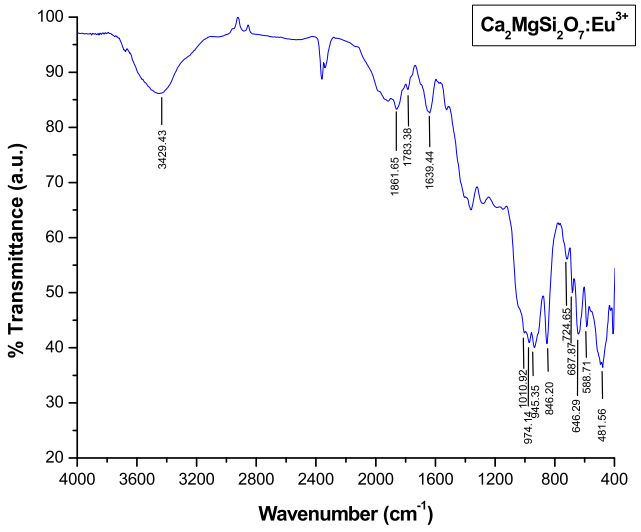

Fig. 5 – FTIR spectra of $Ca_2MgSi_2O_7:Eu^{3+}$ phosphor.

carbonation of the samples preparation [$CaCO_3$ (raw material)]. The free CO_3^{2-} ions has a D3h symmetry (trigonal planar) and its spectrum is dominated by the band at 1900–1700 cm^{-1}. The vibration band of 1639.44 cm^{-1} are assigned due to the Mg^{2+} and bending of the sharp peaks in the region of 846.20 and 724.65 cm^{-1} are assigned due to Ca^{2+}. When Eu^{3+} enters the lattice, it will replace the Ca^{2+} in the $Ca_2MgSi_2O_7$ host and occupy Ca^{2+} lattice sites due to distortion in the $Ca_2MgSi_2O_7$ host crystal lattice. Original position of Ca^{2+} was replaced by Eu^{3+} and the original of Ca^{2+} located at somewhere. Therefore the vibration mode of Ca^{2+} at 846.20 and 724.65 cm^{-1} is clearly observed from $Ca_2MgSi_2O_7$:Eu^{3+} phosphor (Chang & Mao, 2005, Sahu, Bisen, & Brahme, 2014c).

According to the crystal structure of $Ca_2MgSi_2O_7$, the coordination number of calcium can be 6 and 8. Therefore, Ca^{2+} can occupy two alternative lattice sites, the six coordinated Ca^{2+} site [CaO_6 (Ca (I) site)] and the eight coordinated Ca^{2+} site [CaO_8 (Ca (II) site)], and other two independent cations sites, namely Mg^{2+} [MgO_4], and Si^{4+} [SiO_4] also exist in the crystal lattice. Mg^{2+} and Si^{4+} cations occupy in the tetrahedral sites. Eu^{3+} ions can occupy with 3 oxidation state (3, 2 and 1) and five alternative lattice sites. The coordination number of europium can be 6, 7, 8, 9 and 10 (Eu (I), Eu (II), Eu (III), Eu (IV) and Eu (V), respectively) (Vicentini, Zinner, Zukerman-Schpector, & Zinner, 2000). It's hard for Eu^{3+} ions to incorporate the tetrahedral [MgO_4] or [SiO_4] symmetry but it can easily incorporate hexahedral [CaO_6] or octahedral [CaO_8]. Another fact that supports that the radius of Eu^{3+} (1.07 Å) are very close to that of Ca^{2+} (about 1.12 Å) rather than Mg^{2+} (0.65 Å) and Si^{4+} (0.41 Å). Therefore, the Eu^{3+} ions are expected to occupy the Ca^{2+} sites in the $Ca_2MgSi_2O_7$:Eu^{3+} phosphor (Chandrappa, Ghosh, & Patil, 1999; Salim et al. 2009).

3.6. *Photoluminescence (PL)*

The excitation spectrum of $Ca_2MgSi_2O_7$:Eu^{3+} phosphor monitored at 593 nm emission is given in Fig. 6(a). The spectrum of $Ca_2MgSi_2O_7$:Eu^{3+} phosphor exhibit a broad band in the UV region centered at about 265 nm, and several sharp lines between 300 to 400 nm. It can be seen from Fig. 6(a), the excitation spectrum is composed of two major parts: (1) the broad band between 220 and 300 nm, the broad absorption band is called charge transfer state (CTS) band due to the europium–oxygen interactions, which is caused by an electron transfer from an oxygen 2p orbital to an empty 4f shell of europium and the strongest excitation peak is at about 265 nm. (2) A series of sharp lines between 300 and 400 nm, ascribed to the f–f transition of Eu^{3+}. The strongest sharp peak is located at 395 nm corresponding to $^7F_0 \rightarrow {}^5L_6$ transition of Eu^{3+}. Other weak excitation peaks are located at 319, 363 and 383 nm are related to the intra-configurational 4f–4f transitions of Eu^{3+} ions in the host lattices, which can be assigned to $^7F_0 \rightarrow {}^5H_6$, $^7F_0 \rightarrow {}^5D_4$ and $^7F_0 \rightarrow {}^5L_7$ transitions, respectively. The prepared $Ca_2MgSi_2O_7$:Eu^{3+} phosphor can be excited by near UV (NUV) at about 395 nm effectively. So, it can match well with UV and NUV-LED, showing a great potential for practical applications (Wu, Hu, Wang, Kang, & Mou, 2011, Sahu, Bisen, & Brahme, 2014d).

Fig. 6(b) shows the emission spectra of $Ca_2MgSi_2O_7$:Eu^{3+} phosphor in the range of 475–700 nm. Under the 395 nm excitation, the emission spectrum of our obtained samples was composed of a series of sharp emission lines, corresponding to transitions from the excited states $^5D_0$ to the ground state $^7F_{j\ (j\ =\ 0,1,2,3)}$. The orange emission at about 593 nm belongs to the magnetic dipole $^5D_0 \rightarrow {}^7F_1$ transition of Eu^{3+}, and the transition hardly varies with the crystal field strength. The red emission at 615 nm ascribes to the electric dipole $^5D_0 \rightarrow {}^7F_2$ transition of Eu^{3+}, which is very sensitive to the local environment around the Eu^{3+}, and depends on the symmetry of the crystal field. It is found that the 593 and 615 nm emissions are the two strongest peaks, indicating that there are two Ca^{2+} sites in the $Ca_2MgSi_2O_7$ lattice. One site, Ca (I), is inversion symmetry and the other site, Ca (II), is non-inversion symmetry. When doped in $Ca_2MgSi_2O_7$ the Eu^{3+} ions occupied the two different sites of Ca (I) and Ca (II). Other two emission peaks located at 580 and 652 nm are relatively weak, corresponding to the $^5D_0 \rightarrow {}^7F_0$ and $^5D_0 \rightarrow {}^7F_3$ typical transitions of Eu^{3+} ions respectively (Kuang et al. 2014, Sahu, Bisen, & Brahme, 2014d).

For the phosphor $Ca_2MgSi_2O_7$:Eu^{3+} prepared in our experiment, the strongest orange emission peak is located at

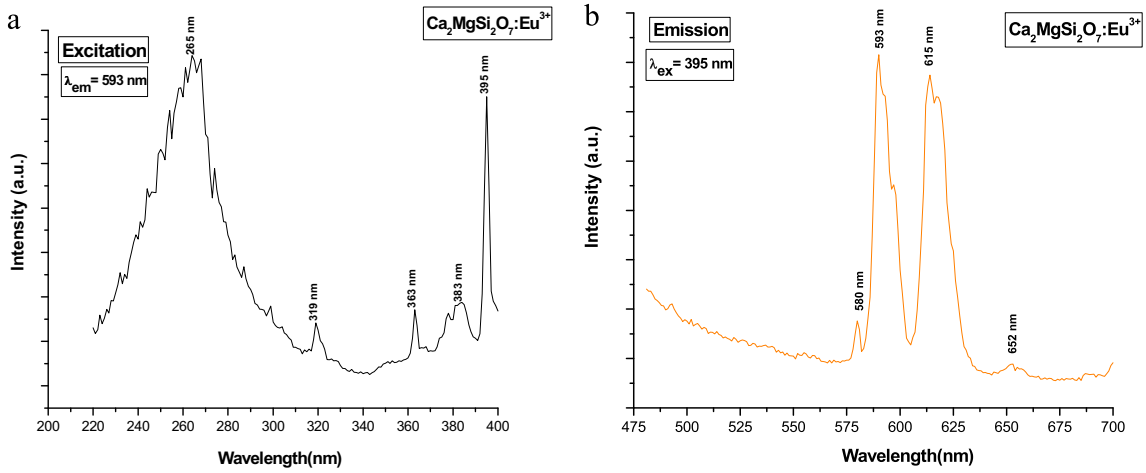

Fig. 6 – (a) Excitation spectra of $Ca_2MgSi_2O_7$:Eu^{3+} phosphor. (b) Emission spectra of $Ca_2MgSi_2O_7$:Eu^{3+} phosphor.

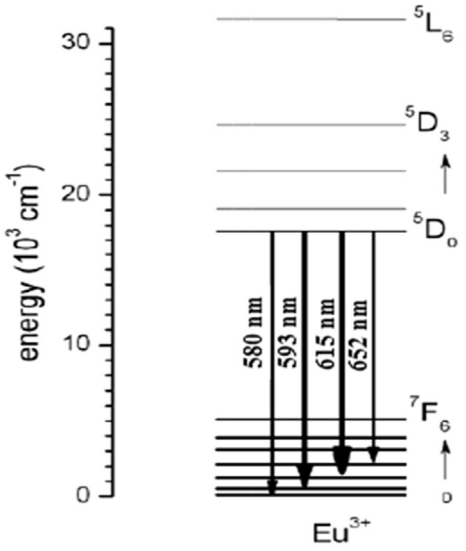

Fig. 7 – Schematic energy level diagram of $Ca_2MgSi_2O_7:Eu^{3+}$ phosphor.

593 nm will be dominated. It can be presumed that Eu^{3+} ions mainly occupy with an inversion symmetric center in host lattice. Fig. 7 shows the schematic energy level diagram of Eu^{3+} ions in the $Ca_2MgSi_2O_7$ host depicting different emissions bands.

3.7. *Long afterglow (decay)*

Fig. 8 shows the typical decay curves of $Ca_2MgSi_2O_7:Eu^{3+}$ phosphor. The initial afterglow intensity of the sample was high. The decay times of $Ca_2MgSi_2O_7:Eu^{3+}$ phosphor can be calculated by the curve fitting technique, and the decay curves fitted by the single exponential components have different decay times.

$$I = I_0 \exp(-t/\tau) \quad (1)$$

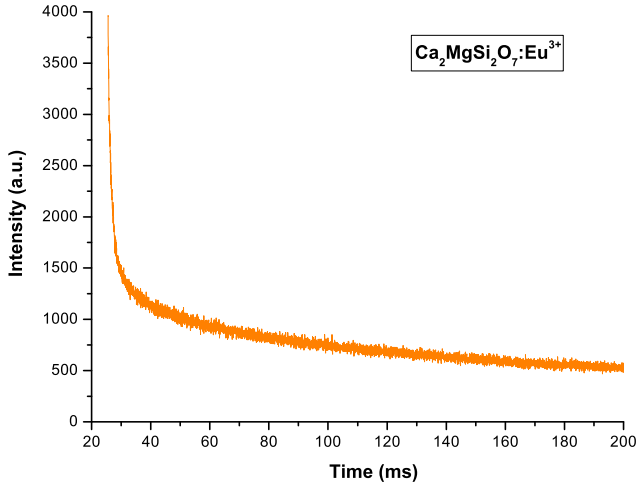

Fig. 8 – Decay Curve of $Ca_2MgSi_2O_7:Eu^{3+}$ phosphor.

Table 1 – Fitting results of the decay curves.

Phosphor	τ (ms)
$Ca_2MgSi_2O_7:Eu^{3+}$	28.47

where, I_0 and I are the luminescence intensities at time 0 and t, respectively, and τ is the luminescence lifetime. Based on the decay curve and the above mentioned Eq. (1) the fitting curve result are shown in Table 1.

As it was reported before (Hong et al. 2011), when Eu^{3+} ions were doped into $Ca_2MgSi_2O_7$, they would substitute the Ca^{2+} ions. To keep electro-neutrality of the compound, two Eu^{3+} ions would substitute three Ca^{2+} ions. The process can be expressed as

$$2Eu^{3+} + 3Ca^{2+} \rightarrow 2[Eu_{Ca}]^{*} + [V_{Ca}]''$$

Each substitution of two Eu^{3+} ions would create two positive defects of $[Eu_{Ca}]^*$ capturing electrons and one negative vacancy of $[V_{Ca}]''$. These defects act as trapping centers for charge carriers. Then the vacancy $[V_{Ca}]''$ would act as a donor of electrons while the two $[Eu_{Ca}]^*$ defects become acceptors of electrons. By thermal stimulation, electrons of the $[V_{Ca}]''$ vacancies would then transfer to the Eu^{3+} sites. The results indicate that the depth of the trap is too shallow leading to a quick escape of charge carriers from the traps resulting in a fast recombination rate in milliseconds (ms).

3.8. *CIE chromaticity coordinate*

In general, color of any phosphor material is represented by means of color coordinates. The luminescence color of the samples excited under 395 nm has been characterized by the CIE (Commission International de l'Eclairage) 1931

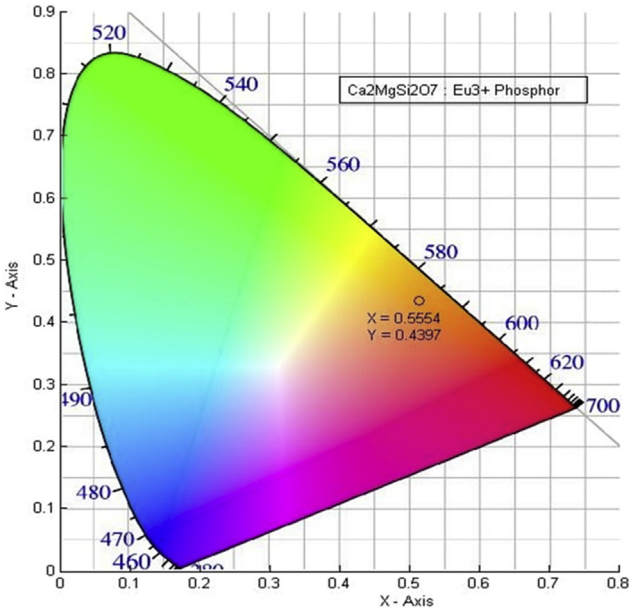

Fig. 9 – CIE chromaticity diagram of $Ca_2MgSi_2O_7:Eu^{3+}$ phosphor.

chromaticity diagram. The emission spectrum of the Eu^{3+} doped $Ca_2MgSi_2O_7$ phosphor was converted to the CIE 1931 chromaticity using the photoluminescent data and the interactive CIE software (CIE coordinate calculator) diagram as shown in Fig. 9 (Sahu, Bisen, & Brahme, 2014a).

Every natural color can be identified by (X, Y) coordinates that are disposed inside the 'chromatic shoe' representing the saturated colors. Luminescence colors of Eu^{3+} doped $Ca_2MgSi_2O_7$ phosphor are placed in the orange-red (X = 0.5554, Y = 0.4397) corners. The chromatic co-ordinates of the luminescence of this phosphor are measure and reached to orange-red luminescence (CIE 1931).

4. Conclusion

A new orange–red emitting phosphor of $Ca_2MgSi_2O_7:Eu^{3+}$ was synthesized by high temperature solid state reaction method at 1200 °C and its photoluminescence properties were investigated. The EDX spectra confirm the present elements in $Ca_2MgSi_2O_7:Eu^{3+}$ phosphor. The excitation spectra indicate the phosphor can be effectively excited by near ultraviolet (NUV) light, making it attractive as conversion phosphor for LED applications. The $Ca_2MgSi_2O_7:Eu^{3+}$ phosphor exhibits bright orange–red emission excited by 395 nm. Photoluminescence measurements showed that the phosphor exhibited emission peak with good intensity at 593 nm, corresponding to $^5D_0 \rightarrow {}^7F_1$ orange emission and weak $^5D_0 \rightarrow {}^7F_2$ red emission. The band at 395 nm can be assigned to $^7F_0 \rightarrow {}^5L_6$ transition of Eu^{3+} ions due to the typical f–f transitions within Eu^{3+} of $4f^6$ configuration. CIE chromaticity diagram confirms $Ca_2MgSi_2O_7:Eu^{3+}$ phosphor exhibits efficient orange–red emission and excellent color stability, indicating that it has favorable properties for application as near ultraviolet LED conversion phosphor.

Acknowledgment

"We are very grateful to UGC-DAE Consortium for Scientific Research, Indore (M.P.) for the XRD Characterization and we are very thankful Dr. Mukul Gupta for his co-operation". We are very thankful to Dr. K.V.R. Murthy, Department of Applied physics, M.S. University Baroda, Vadodara (Gujarat) India for the photoluminescence study.

REFERENCES

Chandrappa, G. T., Ghosh, S., & Patil, K. C. (1999). Synthesis and properties of Willemite, Zn_2SiO_4, and $M^{2+}:Zn_2SiO_4$ (M = Co and Ni). *Journal of Materials Synthesis and Processing, 7*, 273–279.

Chang, C., & Mao, D. (2005). Luminescent properties of $Sr_2MgSi_2O_7$ and $Ca_2MgSi_2O_7$ long lasting phosphors activated by Eu^{2+}, Dy^{3+}. *Journal of Alloy and Compound, 390*, 133–137.

CIE (1931). International Commission on Illumination. Publication CIE no. 15 (E-1.3.1).

Dong, X., Zhang, J., Zhang, X., Hao, Z., & Luo, Y. (2014). New orange–red phosphor $Sr_9Sc(PO_4)_7:Eu^{3+}$ for NUV-LEDs application. *Journal of Alloys and Compounds, 587*, 493–496.

Gorller-Walrand, C., Fluyt, L., Ceulemans, A., & Carnall, W. T. (1995). Magnetic dipole transitions as standards for Judd–Ofelt parametrization in lanthanide spectra. *Journal of Chemical Physics, 1991*, 3099–3106.

Gou, Z., Chang, J., & Zhai, W. (2005). Preparation and characterization of novel bioactive dicalcium silicate ceramics. *Journal of the European Ceramic Society, 25*, 1507–1514.

Hong, Y., Guimei, G., Li, K., Guanghuan, L., Shucai, G., & Guangyan, H. (2011). Synthesis and luminescence properties of a novel red-emitting phosphor $SrCaSiO_4:Eu^{3+}$ for ultraviolet white light-emitting diodes. *Journal of Rare Earths, 29*(5), 431–435.

Jiao, H. Y., & Wang, Y. (2012). A potential red-emitting phosphor $CaSrAl_2SiO_7:Eu^{3+}$ for near ultraviolet light emitting diodes. *Physica B, 407*, 2729–2733.

Kuang, S. P., Liang, K., Liu, J., Mei, Y. M., Jiang, M., Wu, Z. C., et al. (2014). Preparation and photoluminescence properties of a new orange–red $Ba_3P_4O_{13}:Eu^{3+}$ phosphor. *Optik – International Journal for Light and Electron Optics*. http://dx.doi.org/10.1016/j.ijleo.2013.12.037.

Liu, J., Liang, K., Wu, Z. C., Mei, Y. M., Kuang, S. P., & Li, D. X. (2014). The reduction of Eu^{3+} to Eu^{2+} in a new orange–red emission $Sr_3P_4O_{13}$:Eu phosphor prepared in air and its photoluminescence properties. *Ceramics International, 40*, 8827–8831.

Sahu, I. P., Bisen, D. P., & Brahme, N. (2014a). Dysprosium doped di-strontium magnesium di-silicate White light emitting phosphor by solid state reaction method. *Displays, 35*, 279–286.

Sahu, I. P., Bisen, D. P., & Brahme, N. (2014b). Structural characterization and optical properties of $Ca_2MgSi_2O_7:Eu^{2+},Dy^{3+}$ phosphor by solid-state reaction method. *Lumiescence:The Journal of Biological and Chemical Luminescence*. http://dx.doi.org/10.1002/bio.2771 (Wiley publication).

Sahu, I. P., Bisen, D. P., & Brahme, N. (2014c). Luminescence properties of Eu^{2+} and Dy^{3+} doped $Sr_2MgSi_2O_7$ and $Ca_2MgSi_2O_7$ phosphors by solid state reaction method. *Research on Chemical Intermediates*. http://dx.doi.org/10.1007/s11164-014-1767-6 (Springer publication).

Sahu, I. P., Bisen, D. P., & Brahme, N. (2014d). Photoluminescence properties of europium doped di-strontium magnesium di-silicate phosphor by solid state reaction method. *Journal of Radiation Research and Applied Sciences, 8*(1), 104–109. http://dx.doi.org/10.1016/j.jrras.2014.12.006.

Sahu, I. P., Bisen, D. P., & Brahme, N. (2015a). Luminescence properties of Green emitting $Ca_2MgSi_2O_7:Eu^{2+}$ phosphor by solid state reaction method. *Lumiescence: The Journal of Biological and Chemical Luminescence*. http://dx.doi.org/10.1002/bio.2869 (Wiley publication).

Sahu, I. P., Bisen, D. P., Brahme, N., Wanjari, L., & Tamrakar, R. K. (2015b). Structural characterization and luminescence properties of Bluish-Green emitting $SrCaMgSi_2O_7:Eu^{2+}$, Dy^{3+} phosphor by solid state reaction method. *Research on Chemical Intermediates*. http://dx.doi.org/10.1007/s11164-015-1929-1 (Springer publication).

Sahu, I. P., Bisen, D. P., Brahme, N., & Ganjir, M. (2015c). Enhancement of the photoluminescence and long afterglow properties of $Sr_2MgSi_2O_7:Eu^{2+}$ phosphor by Dy^{3+} co-doping. *Lumiescence: The Journal of Biological and Chemical Luminescence*. http://dx.doi.org/10.1002/bio.2900 (Wiley publication).

Salim, M. A., Hussain, R., Abdullah, M. S., Abdullah, S., Alias, N. S., & Ahmad Fuzi, S. A. (2009). The local structure of phosphor material, $Sr_2MgSi_2O_7$ and $Sr_2MgSi_2O_7:Eu^{2+}$ by infrared spectroscopy. *Solid State Science and Technology, 17*, 59–64.

Shrivastava, R., & Kaur, J. (2014). Studies on long lasting optical properties of europium and dysprosium doped di-strontium magnesium silicate phosphors. *Indian Journal of Physics*. http://dx.doi.org/10.1007/s12648-014-0535-1.

Talwar, G. J., Joshi, C. P., Moharil, S. V., Dhopte, S. M., Muthal, P. L., & Kondawat, V. K. (2009). Combustion synthesis of $Sr_3MgSi_2O_8:Eu^{2+}$and $Sr_2MgSi_2O_7:Eu^{2+}$phosphors. *Journal of Luminescence, 129*(11), 1239.

Vicentini, G., Zinner, L. B., Zukerman-Schpector, J., & Zinner, K. (2000). Luminescence and structure of europium compounds. *Coordination Chemistry Reviews, 196*, 353–382.

Wang, Z., Lou, S., & Li, P. (2014). Enhanced orange–red emission of $Sr_3La(PO_4)_3:Ce^{3+}$,Mn^{2+} via energy transfer. *Journal of Luminescence, 156*, 87–90.

Wu, H., Hu, Y., Wang, Y., Kang, F., & Mou, Z. (2011). Investigation on Eu^{3+} doped $Sr_2MgSi_2O_7$ red emitting phosphors for white light emitting diodes. *Optics & Laser Technology, 43*, 1104–1110.

Xu, M., Wang, L., Liu, L., Jia, D., & Sheng, R. (2014). Influence of Gd^{3+} doping on the luminescent of $Sr_2P_2O_7:Eu^{3+}$ orange–red phosphors. *Journal of Luminescence, 146*, 475–479.

Yang, H. K., Moona, B. K., Choi, B. C., Jeong, J. H., & Kim, K. H. (2012). Crystal growth and photoluminescence characteristics of $Ca_2MgSi_2O_7:Eu^{3+}$ thin films grown by pulsed laser deposition. *Materials Research Bulletin, 47*, 2871–2874.